Journal of Applied Polymer Science

Flame Retardancy and Mechanical Properties of Polyamide 6 with Melamine Polyphosphate and Ionic Liquid Surfactant-Treated Montmorillonite

Ri-Chao Zhang,[1] Soon Man Hong,[1,2] Chong Min Koo[1,2]

[1]Center for Materials Architecturing, Korea Institute of Science and Technology, Hwarangno 14-gil 5, Seongbuk-gu, Seoul 136-791, Republic of Korea

[2]Nanomaterials Science and Engineering, University of Science and Technology, 176 Gajung-dong, 217 Gajungro, Yuseong-gu, Daejeon 305-350, Republic of Korea

Correspondence to: C. M. Koo (E-mail: koo@kist.re.kr)

ABSTRACT: The mechanical properties and inflammability of polyamide 6 (PA6) nanocomposites incorporated with Montmorillonite organoclay (MMT) modified with thermal stable ionic liquid surfactants were investigated. The compatibility between ionic liquid-treated MMT and PA6 matrix was improved and the intercalation morphology was achieved, which resulted in the increaseof tensile modulus. However, the addition of organo-MMTs alone did not improve the inflammability of the PA6 nanocomposite, because of strong melt-dripping behavior of PA6 matrix. Addition of auxiliary melamine polyphosphate (MPP) intumescent flame retardant to the nanocomposite prevented the melt dripping and enhanced inflammability performance. The enhanced inflammability of PA6/organoclay/MPP nanocomposites was attributed to the synergistic effect between imidazolium or phosphonium organo-MMTs and intumescent flame retardant MPP. © 2014 Wiley Periodicals, Inc. J. Appl. Polym. Sci. **2014**, *131*, 40648.

KEYWORDS: composites; flame retardance; polyamides

Received 27 October 2013; accepted 27 February 2014
DOI: 10.1002/app.40648

INTRODUCTION

Polymer layered clay nanocomposites have attracted intense academic and industrial interest because great improvement in mechanical and barrier properties can be achieved even at very small clay content.[1–9] Enhancement of these properties markedly depends on extent of dispersion of layered clays, for example montmorillonite (MMT), in the polymer matrix.[10,11] Therefore, it is important to disperse homogeneously the layered clay in the polymer matrix. Indeed, two ideal and homogen polymer–clay nanocomposites are possible: intercalated and exfoliated. Intercalation results from the penetration of polymer chains into the gallery of layered clay, while in the exfoliation, the single nanometer-thick silicate platelets are randomly dispersed in the polymer matrix. Exfoliated polymer nanocomposites usually provide the best mechanical properties because of the large aspect ratio and surface area of silicate platelet dispersion.

Considering the hydrophilic character of natural clays, which makes them inherently incompatible with most organic polymers, it is very important to modify the clay with an organic surfactant to make it compatible with polymer and improve the dispersion of the clay in the matrix. In the past decades, a lot of efforts were devoted towards improving compatibility between clay and polymer and dispersion of clay in polymer matrix through using conventional organic surfactants, such as alkyl ammoniums.[12–17] However, the organoclays modified with conventional ammonium surfactants start to decompose at ~200°C below the melt processing temperature of most polymers, implying that the alkyl ammonium surfactant would degrade during compounding.[18–20] Thus, a great effort has been made to modify the clay with thermally stable organic surfactants to improve its thermal stability.[21–26] Gilman et al.[21] initially reported that alkyl imidazolium modified clay revealed the onset decomposition temperature of 100°C above that of conventional ammonium modified organoclay. Wilkie et al.[22] also synthesized the organoclay with highly thermally stable benzimidazolium surfactant that degraded at about 300°C, and observed better thermal stability of styrenic polymer nanocomposite when using the benzimidazolium organoclay.

Regarding inflammability, most polymer–organoclay binary nanocomposites could not pass the ignition resistance tests, such as UL-94 vertical burning, even at quite large organoclay content of 30 wt %.[27–32] Many polymer–organoclay-flame retardant ternary nanocomposites, including commonly used

Sample	Chemical structure
PA6	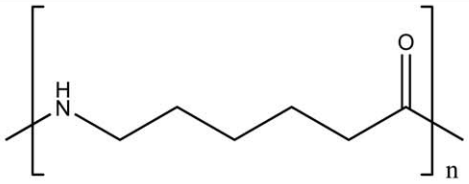
ICF_3SO_3	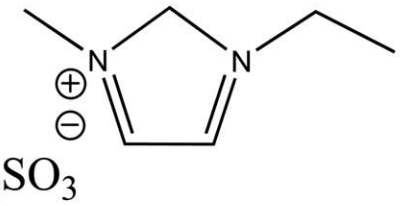
DPPBr	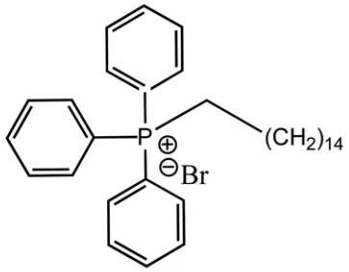
DOPBr	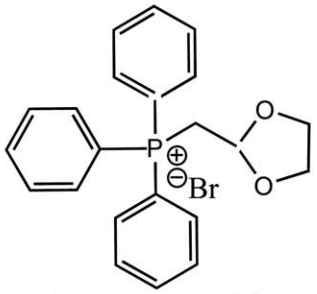
MPP	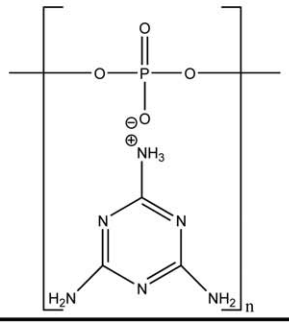

Scheme 1. Chemical structures of PA6, three surfactants and MPP.

flame retardants, were investigated to enhance the inflammable property of polymer nanocomposites. However, the inflammable efficiency of flame retardants in polymer nanocomposites deteriorated with the addition of organoclay. For example, Hu et al.[31] prepared PA6 nanocomposites with ammonium organoclay and micron-sized melamine cyanurate (MCA) and observed that PA6 with 15 wt % MCA reached V0 rating, whilst the addition of ammonium organoclay in PA6/MCA composite deteriorated its inflammable property in the UL-94 vertical burning test. Zhang et al.[33] reported that the flame retardant efficiency of melamine was damaged with 1 wt % of organoclay in polymer nanocomposites. Recently, Sheng et al.[34] reported that the flame retardancy of PA66 nanocomposite also reduced with addition of organoclay modified with thermally stable immidazolium surfactants.

In the present work, we prepared thermally stable organoclay modified with three different kinds of ionic liquid surfactants and fabricated PA6/organoclay nanocomposites via melt extrusion. To improve the flame retardancy of PA6 nanocomposites, an intumescent flame retardant, melamine polyphosphate (MPP), was added to the PA6-organoclay nanocomposites during melt extrusion. The morphology, thermal stability,

mechanical and inflammability properties of the melt-extruded and compression-molded PA6/organo clay nanocomposites were investigated to reveal the synergistic effect of organoclay and MPP blends.

EXPERIMENTAL

Materials

PA6 with a trade name of V32412 and melting temperature of 224°C was supplied from KP Chemtech, Republic of Korea. Sodium-montmorillonite (Na^+–MMT, Cloisite Na^+) with cation exchange capacity (CEC) of 92 meq/100g was provided by Southern Clay, USA. Ionic liqud, 1-ethyl-3-methylimidazolium trifluoromethanesulfonate (ICF_3SO_3), was obtained from C-TRI, Republic of Korea. Both (1,3-dioxolan-2-ylmethyl)triphenylphosphonium bromide (DOPBr) and dodecyltriphenylphosphonium bromide (DPPBr) were purchased from Aldrich, USA. Melamine polyphosphate (MPP), a typical intumescent flame retardant supplied from Budit3141, Spain, was used as an auxiliary flame retardant. The chemical structures of PA6, three surfactants and MPP are presented in Scheme 1. All materials were used as received.

Ionic Liquid Modification of MMT

The organoclays were prepared through cation exchange of the Na^+–MMT with three different thermally stable surfactants (ionic liquid): ICF_3SO_3, DOPBr, and DPPBr. 5 g of Na^+–MMT was dispersed in 1000 mL of deionized water and stirred with a magnetic stirrer for 24 h at 80°C. The amount of surfactant added to the solution was equivalent to 2 CEC, based on the cation exchange capacity (CEC = 92 meq/100 g) of MMT. The dispersions were stirred vigorously at 80°C for 24 h. The modified MMT was filtered and washed with distilled water until no residual halogen anions were detected using an aqueous silver nitrate ($AgNO_3$). The resulting organo-MMT was dried at 80°C for 24 h under vacuum and then was ground into fine powder. The following abbreviations were used as designing the different organo-MMTs: IMMT representing the organo-MMT modified with ICF_3SO_3 imidazolium surfactant, DPPMMT and DOPMMT for organo-MMTs modified with DPPBr and DOPBr phosphonium surfactants, respectively.

Preparation of Nanocomposites

Two series of PA6 nanocomposites were prepared via melt extrusion process. The first series of nanocomposites contained only PA6 and clay. The second series, in addition to PA6, included clay and intumescent flame retardant MPP. Four different clay, including MMT, IMMT, DPPMMT, and DOPMMT, were used as clay. Clay and MPP contents were fixed at 5 and 60 phr, respectively. PA6 pellets, IMMT, DPPMMT, DOPMMT, and MPP were dried at 80°C for 24 h before melt compounding. The PA6 nanocomposites were prepared in a single-screw extruder with rotor speed of 50 rpm at 250°C. The extrudates were dried in a vacuum oven for 24 h and compression-molded into rectangular bars (63 mm × 12.5 mm × 3 mm) for UL-94 vertical burning tests and limiting oxygen index (LOI) measurements. Dumbbell-like bars with a gauge length of 12 mm for uniaxial tensile examinations were also prepared using a laboratory press at 250°C. The compositions of the prepared nanocomposites are given in Table I.

Table I. Compositions of the Prepared Compounds

Components	Weight ratio
PA6	1
PA6 : MMT	20 : 1
PA6 : IMMT	20 : 1
PA6 : DPPMMT	20 : 1
PA6 : DOPMMT	20 : 1
PA6 : MPP	20 : 12
PA6 : MPP : MMT	20 : 12 : 1
PA6 : MPP : IMMT	20 : 12 : 1
PA6 : MPP : DPPMMT	20 : 12 : 1
PA6 : MPP : DOPMMT	20 : 12 : 1

Characterizations

Fourier transform infrared (FTIR) analyses of the samples were conducted with a Thermo Scientific infrared spectrometer, USA. The thermal stability was examined using a thermogravimetric analysis instrument (TGA, Q50 TA Instrument Analyzer, USA). Nearly 10 mg of samples were heated from room temperature to 800°C at a heating rate of 20°C min^{-1} under nitrogen flow. X-ray diffraction (XRD) measurements were carried out using Rigaku D/Max-2500 X-ray powder diffractometer with Cu Kα radiation ($\lambda = 0.15418$ nm) at a generator voltage of 40 kV and a current of 50 mA. The morphologies of the nanocomposites were observed and recorded using transmission electron microscopy (TEM, Tecnai G2/F20 TEM, USA) at an accelerating voltage of 200 kV after ultra-microtoming. Tensile strength and elongation at break were measured using an Instron UTM5567 electromechanical testing system at the crosshead speed of 10 mm min^{-1} at ambient temperature. The LOI measurements were carried out with an ON-10, SUGA test instrument. According to ASTM D 2863 standard method, the sample was held vertically in the glass column chamber in which the flow of oxygen and nitrogen mixture gas was controlled. After ignition, the LOI values of the samples could be obtained through adjusting the oxygen and nitrogen concentrations for burning of the samples.[35] The UL-94 classification of the samples was obtained via vertical burning tester in accordance with ASTM D 3801 standard method. The specimen was vertically fixed at the clip of the stand. Cotton was used as an indicator for the flaming particles or drops, placing 300-mm below the specimen.[35] A burner was used to ignite the samples for 10 s. The ignition was repeated two times. After ignition, the burning time of samples was measured to evaluate the flammable classification.

RESULTS AND DISCUSSION

Characterization of Modified MMT

Figure 1 represents the FTIR spectra of pristine Na^+-MMT, modified MMTs, and surfactants. The pristine MMT provided typical Si—O and Al—O bond vibrations of aluminosilicates at 1044 and 620 cm^{-1} and vibration of hydroxyl groups at 3600 cm^{-1}. After modification with the imidazolium and phosphonium surfactants, new signals appeared in the FTIR spectra of the organo-MMTs. In Figure 1(a), the peak at 1580 cm^{-1} assigned to C—C/C—N stretching vibration and the peaks at 1120 and 720 cm^{-1}, assigned

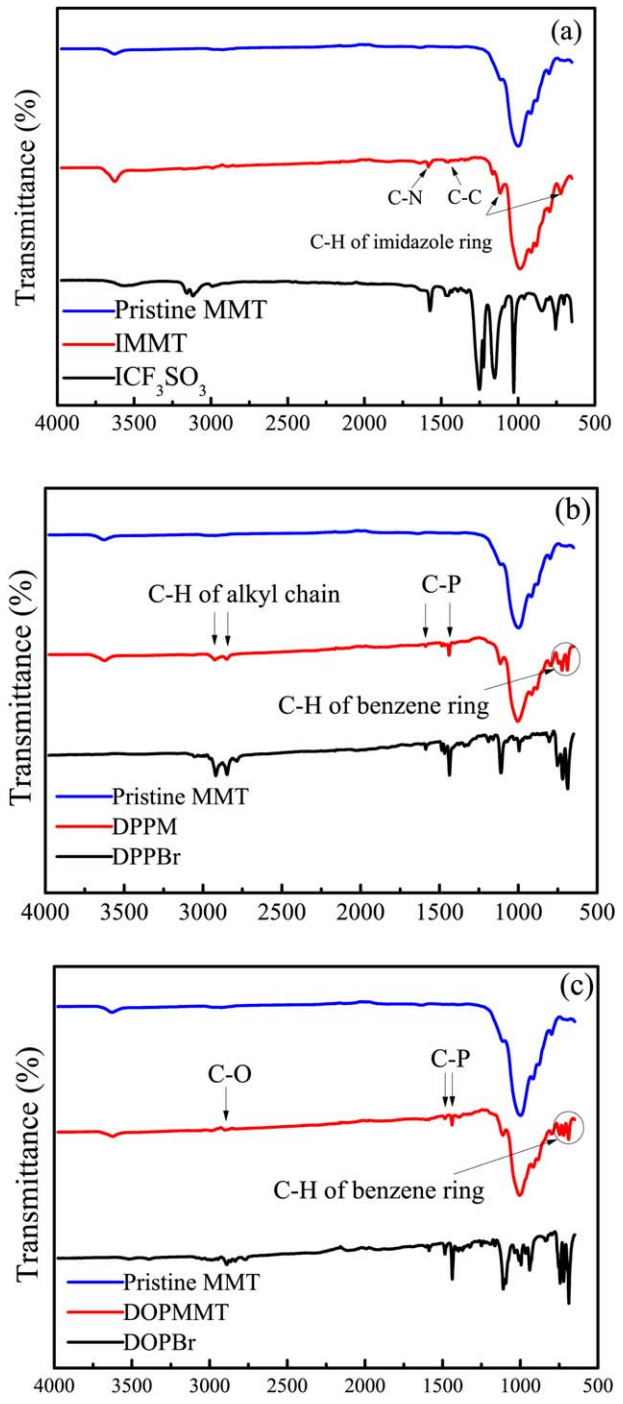

Figure 1. FTIR spectra of pristine MMT, surfactant modified MMT, and surfactant: (a) ICF_3SO_3, (b) DOPBr, (c) DPPBr surfactants were used, respectively. [Color figure can be viewed in the online issue, which is available at wileyonlinelibrary.com.]

to C—H stretching vibration in the imidazole rings for the IMMT, were confirmed. Meanwhile, the same phenomenon was observed for DPPMMT and DOPMMT, as shown in Figure 1(b,c). Both DPPMMT and DOPMMT revealed typical P—C stretching vibrations at 1440 and 1484 cm^{-1}. For DPPMMT, in addition to typical P—C stretching vibrations, the peaks at 689 and 725 cm^{-1}, corresponding to C—H stretching vibrations of

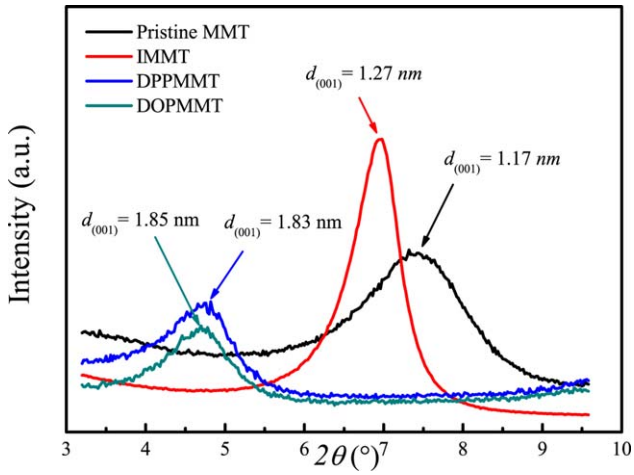

Figure 2. XRD patterns of pristine MMT and MMTs modified with ICF_3SO_3, DOPBr, and DPPBr surfactants. [Color figure can be viewed in the online issue, which is available at wileyonlinelibrary.com.]

benzene ring, and peaks at 2920 and 2850 cm^{-1}, corresponding to C—H stretching vibrations of alkyl chain, were observed in the FTIR spectra [Figure 1(b)]. While for DOPMMT in Figure 1(c), the typical C—O bond vibration peak at 2890 cm^{-1} attributed to dioxolan and the absorbent peaks at 689 and 725 cm^{-1} attributed to the C—H bond vibration of benzene ring were observed. These FTIR results indicated that sodium cations in the pristine MMT were effectively exchanged by ICF_3^+ imidazolium, DPP^+, and DOP^+ phosphonium cations.

The pristine MMT consists of aluminosilicate platelets that are stacked by weak dipolar or van der Waals interactions. The gallery spacing between adjacent aluminosilicate sheets depends on the diameter of cations located in the gallery. The intercalation of big-sized organic surfactants into the gallery of MMT results in a large expansion of interlayer space. Figure 2 shows the XRD patterns of pristine MMT and MMTs modified with three surfactants. Pristine MMT revealed a characteristic (001) reflection peak at $2\theta = 7.4°$. According to Bragg's law ($d = \lambda/2 \sin \theta$), where λ is the wavelength of X-ray (0.154 nm) Na^+-MMT showed a interlayer spacing between silicate layers of $d_{001} = 1.17$ nm. After ion exchange, the surfactant cations replaced Na^+ cation and intercalated into the gallery of MMT, resulting in expansion of d_{001} space due to the increase of cationic diameter. The d_{001} increased from 1.17 to 1.27 nm for IMMT, to 1.83 nm for DPPMMT, and to 1.85 nm for DOPMMT. The latter two phosphonium MMTs had larger expansion ratios than the

Table II. Weight Losses and Organic Contents of Clay and Organoclay

Sample	Weight loss (%)	Organic content from TGA (%)	Organic content from CEC calculation (%)
Pristine MMT	4.86	-	-
IMMT	13.71	8.85	9.2
DPPMMT	30.73	25.87	28.4
DOPMMT	24.23	19.37	24.4

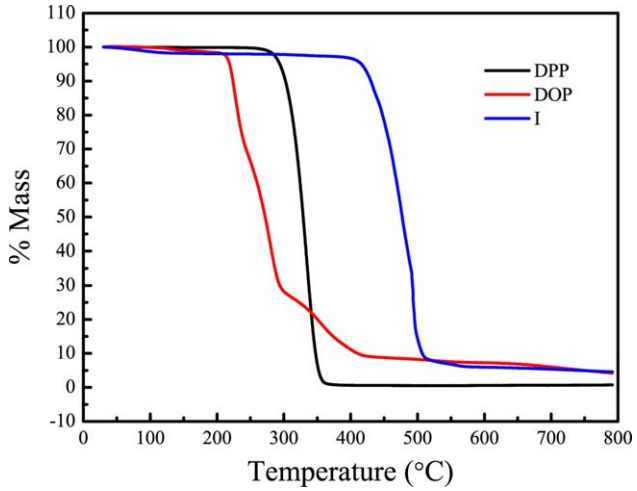

Figure 3. TGA thermograms of ICF3SO_3, DOPBr, and DPPBr surfactants. [Color figure can be viewed in the online issue, which is available at wileyonlinelibrary.com.]

former immidazolium MMT because the phosphonium cations had larger molecular size than the immidazolium cation.

The corresponding loading contents of organic surfactant in organocaly, calculated via TGA experiments and theoretical calculation based on 1 CEC value of each surfactant are listed in Table II. The surfactant contents in the organoclay obtained from TGA examinations were corresponding to the theoretically calculated values based on 1 CEC. They indicate that the most Na^+ cations in the gallery of MMT were fully exchanged by organic imidazolium or phosphonium cations.

Figures 3 and 4 show the thermal stability results of surfactants and organoclays via TGA examinations. The detailed data are summarized in Table III. In Figure 3, DPPBr and DOPBr phosphonium surfactants revealed lower decomposition onset temperatures than ICF_3SO_3 imidazolium surfactant due to the presence of halide anion that decreases the thermal stability of

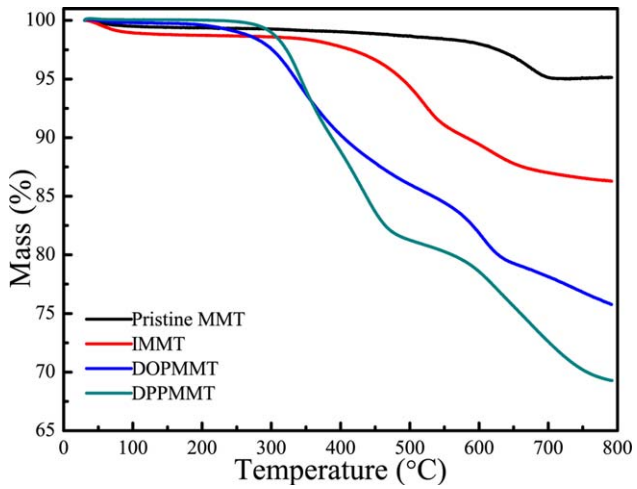

Figure 4. TGA thermograms of pristine MMT and MMTs modified with ICF_3SO_3, DOPBr, and DPPBr surfactants. [Color figure can be viewed in the online issue, which is available at wileyonlinelibrary.com.]

Table III. TGA Results of Surfactant and Organoclay

Sample	Mass loss at 250°C (%)	Temperature at 5% mass loss (°C)	Temperature at max mass loss rate (°C)
ICF_3SO_3	2.1	416	478
IMMT	0.21	489	515
DOPBr	34.7	219	278
DOPMMT	0.72	336	359
DPPBr	0.25	294	329
DPPMMT	0.11	343	444

organic surfactant.[36] Thermal decomposition of DOPBr (temperature at 5% mass loss presented in Table III) started at 200°C, whilst that of ICF_3SO_3 started at 350°C. Although the phosphonium surfactant provided poor thermal stability, the thermal stability of phosphonium MMTs was greatly improved after exchanging ion. According to TGA data (Table III), the onset decomposition temperature of DOPMMT was approximately at 300°C, 100°C above that of DOPBr. Moreover, the mass loss at 250°C was <1% for all of the three organo-MMTs. Thus, the imidazolium and phosphonium organo-MMTs revealed good thermal stability that they did not decompose during the melt-compounding with PA6 at 250°C.

PA6-Organoclay Nanocomposites

Morphology. Generally, the intercalation of organic surfactants into the gallery of MMT reduces the electrostatic effect between adjacent layers as well as the hydrophilicity of the aluminosilicate sheets. This phenomenon allows the polymer chains to penetrate into the interlayers of MMT during melt compounding; thus, resulting in good dispersion of organo-MMT in PA6 matrix. According to XRD patterns of PA6/MMT nanocomposites (Figure 5), the interlayer space of clay increased from 1.17 to 1.34 nm, indicating that PA6 molecular chains incorporated into the galleries of MMT. For the phosphonium and imidazolium PA6/organo-MMT nanocomposites, the d_{001} basal peak

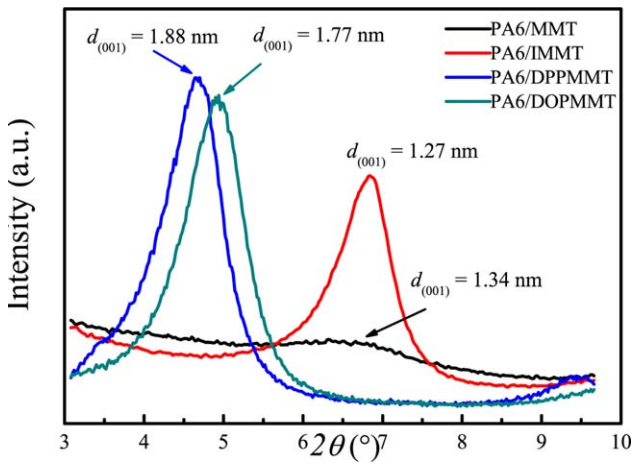

Figure 5. XRD patterns of PA6 nanocomposites with pristine MMT, IMMT, DPPMMT, and DOPMMT. [Color figure can be viewed in the online issue, which is available at wileyonlinelibrary.com.]

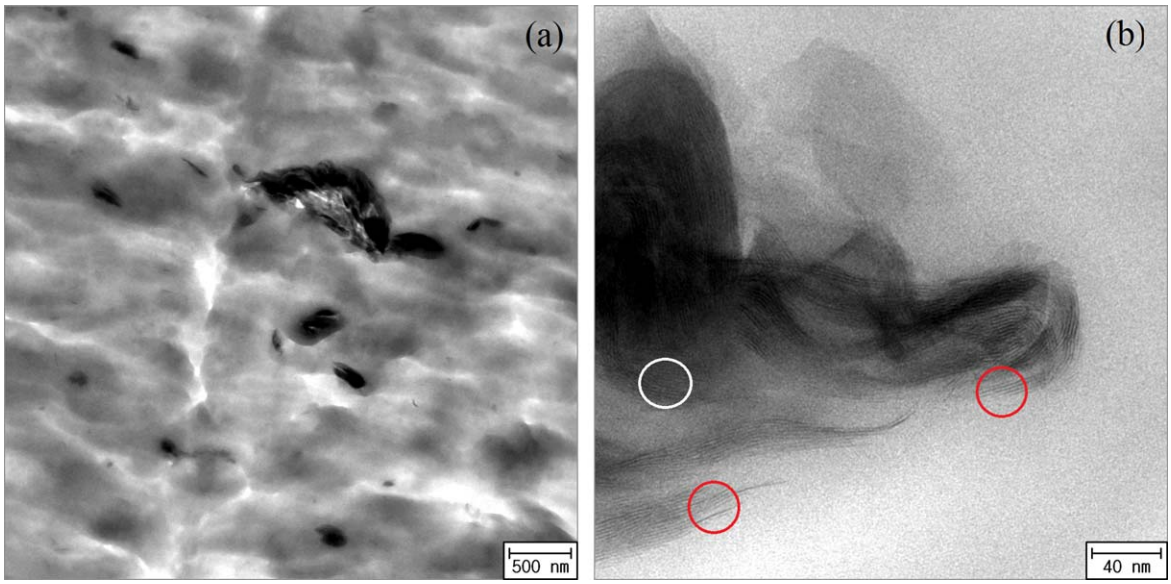

Figure 6. TEM micrographs of PA6/DOPMMT nanocomposite. [Color figure can be viewed in the online issue, which is available at wileyonlinelibrary.com.]

center of organo-MMTs kindly remained the same after melt compounded with PA6. However, the peak distribution was broadened. d_{001} basal spacing distribution of PA6/DPPMMT nanocomposites span in the range of 2.94–1.36 nm (2θ spans 3–6.5°), whereas for DPPMMT d_{001} basal spacing distribution ranges from 2.52 to 1.47 nm (2θ spans 3.5–6°). The change of d_{001} basal spacing distribution could be associated with the fact that the interlayer space of organo-MMTs was partly intercalated with PA6 molecular chains. Figure 6 shows TEM micrographs of PA6/DOPMMT nanocomposites. The smaller magnification TEM micrograph [Figure 6(a)], representing the nanocomposite structure, indicates a generally good clay dispersion of DOPMMT in the PA6 matrix. At larger magnification [Figure 6(b)] an apparent layer stacked structure was observed. The interlayer space of outside layer (red circle part) for the DOPMMT cluster was larger than that of inside layer (white circle part). These TEM observations were in good agreement with the XRD results presented in Figure 5, showing that PA6 molecular chains were partly intercalated into the galleries of organo-MMTs, especially at the outside layers of organo-MMTs.

Mechanical Properties. The mechanical properties of neat PA6 and PA6/organoclay nanocomposites are listed in Table IV. Neat PA6 had tensile modulus of 1272 MPa. The tensile modulus of nanocomposite increased with addition of clay. Modulus of nanocomposite increased 8% by pristine MMT, 6% by IMMT, 11% by DPPMMT, and 15% by addition of DOPMMT. These results were in a good agreement with XRD and TEM observations. The modification of MMT with imidazolium or phosphonium organic surfactants enhanced the compatibility between organoclay and PA6 matrix and dispersion of organoclay particles in the matrix. Good compatibility of organo-MMTs resulted in larger increase in the modulus of PA6 nanocomposite compared with neat MMT. In contrast, the stress at break decreased with addition of clay. The stress at break of nanocomposite decreased 4–36% with addition of organoclays.

Table IV. Tensile and Combustion Properties of PA6 Nanocomposites Containing 60 phr MPP

Sample	Tensile modulus (MPa)	Strain at break (%)	Stress at break (MPa)	LOI (%)	UL-94 rating
PA6	1274	4.7	58	27.5	V2
PA6/MMT	1379	4	54	26.5	V2
PA6/IMMT	1349	4.5	46	28	V2
PA6/DPPMMT	1415	3	41	23.5	V2
PA6/DOPMMT	1481	3	36	27	V2
PA6/MPP	1896	3.3	49	26.5	V2
PA6/MMT/MPP	2077	3	53	38	V0
PA6/IMMT/MPP	2081	2.5	48	31.5	V0
PA6/DPPMMT/MPP	2116	2.4	50	26.5	V0
PA6/DOPMMT/MPP	2072	2.5	48	31	V0

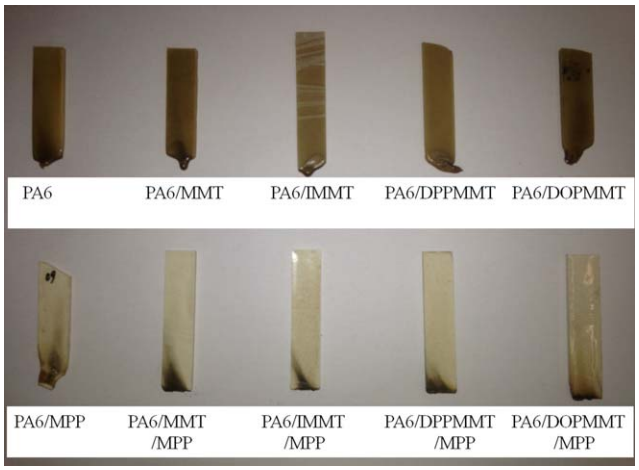

Figure 7. Photographs of neat PA6, PA6/MMT, PA6/IMMT, PA6/DPP, PA6/DOPMMT nanocomposites combined with or without auxiliary flame retardant MPP after UL94 vertical burning tests. [Color figure can be viewed in the online issue, which is available at wileyonlinelibrary.com.]

Interestingly, addition of the intumescent flame retardant MPP strongly enhanced further the tensile modulus, as much as more than 60% in the PA6/DPPMMT/MMT nanocomposites. This strong enhancement could be ascribed to the coordinative effect of MPP between imidazolium or phosphonium surfactant modified MMT and PA6 matrix. Indeed, MPP shows a good compatibility not only with PA6 due to hydrogen bond interaction between PA6 and MPP, but also with imidazolium or phosphonium surfactant modified MMT caused by analogy of chemical structure including phosphonium moiety.[37,38]

Inflammability Properties. Inflammability of PA6 and its nanocomposites were characterized with both UL94 vertical burning test and LOI measurement. The UL94 rating and LOI results of PA6 and its nanocomposites are listed in Table IV. Figure 7 shows photographs of the specimen after UL-94 test. PA6 revealed LOI of 27.5 % and UL-94 rating of V2. PA6/organoclay nanocomposites had slightly decrease in LOI and remained V2 of UL-94 rating. The relatively low melt viscosity of neat PA6 resulted in melt dripping during combustion. The melt drip take away the flame from the bottom of the specimen bars to the cotton on the floor, thus providing V2 rating. Incorporation of organoclay in PA6 was not enough to prevent the melt drip behavior. Thus, incorporation of organoclay hardly improved the inflammability of the nanocomposites.

However, the nanocomposites incorporated with intumescent flame retardant MPP revealed better inflammability, even though the PA6 incorporated with MPP had the same flammability as neat PA6. The LOI value of ternary nanocomposites composed of PA6, organoclay, and MPP unexpectedly increased and the UL94 rating reached V0 with the elimination of melt dripping (Figure 7). MPP decomposes endothermically and releases inert nitrogen that dilutes oxygen and the flammable gases in the flame. Meanwhile, phosphoric acid is also formed as a decomposition product that promotes the formation of insulating char on the surface of polymer.[38,39] However, MPP alone did not increase the flame retardancy of PA6 because the melt dripping still appeared 7). It indicated that although MPP enhanced the formation of insulating char of PA6 after combustion, the charring layer was not enough to prevent the flame extension to the inside part of PA6. Only when MPP was combined with organo-MMTs, the melt dripping was eliminated and UL94 rating reached V0 for PA6 nanocomposites. This might be due to the fact that, during combustion, MPP decomposed, releasing phosphoric acid. The resulting phosphoric acid reacts not only with PA6 to form charred layer but also with MMT to develop a glassy coat. Thus, a densely formed carbonaceous–silicious charred layer insulated the heat and mass transport and prevented the escape of volatile products generated when PA6 was decomposed. As a result, enhanced inflammability of the PA6/organoclay/MPP nanocomposites can be attributed to the synergistic effect between imidazolium or phosphonium organo-MMTs and intumescent flame retardant MPP.

CONCLUSION

Thermally stable organoclays modified with three different kinds of ionic liquid surfactants (ICF_3SO_3, DOPBr, and DPPBr) and PA6/organoclay nanocomposites were fabricated via melt extrusion. The modification of MMT with ionic liquid improved the compatibility between MMT and PA6 matrix which resulted in the increase of tensile modulus of composites, however, the ionic liquid-treated MMT alone failed to enhance the inflammability of the PA6 nanocomposite, because of strong melt-dripping behavior of PA6 matrix. PA6/organoclay/MPP nanocomposites revealed improvement in tensile modulus as well as enhanced flame retardancy compared with PA6 and PA6/organoclay nanocomposites, due to the strong synergistic effect between organoclay and intumescent flame retardant MPP.

ACKNOWLEDGMENTS

This work was financially supported by a program of the World Premium Materials of the Ministry of Knowledge Economy and partially by Korea Institute of Science and Technology. Ri-Chao Zhang also thanks for the financial support from the National Natural Science Foundation of China (51203135).

REFERENCES

1. Ray, S. S.; Okamoto, M. *Prog. Polym. Sci.* **2003**, *28*, 1539.
2. Alexandre, M.; Dubois, P. *Mater. Sci. Eng.* **2000**, *28*, 1.
3. Le Pluart, L.; Duchet, J.; Sautereau, H. *Polymer* **2005**, *46*, 12267.
4. Ait-Hocine, N.; Mederic, P.; Aubry, T. *Polym. Test.* **2008**, *27*, 330.
5. Osman, M. A.; Mittal, V.; Morbidelli, M.; Suter, U. W. *Macromolecules* **2003**, *36*, 9851.
6. Alexandre, B.; Langevin, D.; Mederic, P.; Aubry, T.; Couderc, H.; Nguyen, Q. T.; Saiter, A.; Marais, S. *J. Membr. Sci.* **2008**, *328*, 186.
7. Koo, C. M.; Kim, J. H.; Wang, K. H.; Chung, I. J. *J. Polym. Sci. B* **2005**, *43*, 158.
8. Koo, C. M.; Kim, S. O.; Chung, I. J. *Macromolecules* **2003**, *36*, 2748.

9. Koo, C. M.; Ham, H. T.; Choi, M. H.; Kim, S. O.; Chung, I. J. *Polymer* **2003**, *44*, 681.
10. Mederic, P.; Le Pluart, L.; Aubry, T.; Madec, P. J. *J. Appl. Polym. Sci.* **2013**, *127*, 879.
11. Koo, C. M.; Kim, M. J.; Choi, M. H.; Kim, S. O.; Chung, I. J. *J. Appl. Polym. Sci.* **2003**, *88*, 1526.
12. Dennis, H. R.; Hunter, D. L.; Chang, D.; Kim, S.; White, J. L.; Cho, J. W.; Paul, D. R. *Polymer* **2001**, *42*, 9513.
13. Lertwimolnun W., Vergnes B. Influence of screw profile and extrusion conditions on the microstructure of polypropylene/organoclay nanocomposites. *Polym. Eng. Sci.* **2007**, *47*, 2100.
14. Mederic, P.; Aubry, T.; Razafinimaro, T. *Int. Polym. Proc.* **2009**, *24*, 261.
15. Lee, S. Y.; Cho, W. J.; Kim, K. J.; Ahn, J. H.; Lee, M. *J. Colloid. Interface Sci.* **2005**, *284*, 667.
16. He, H.; Duchet, J.; Galy, J.; Gerard, J. F. *J. Colloid. Interface Sci.* **2006**, *295*, 202.
17. Kord, B. *J. Appl. Polym. Sci.* **2011**, *120*, 607.
18. Xie, W.; Gao, Z.; Pan, W.; Hunter, D.; Singh, A.; Vaia, R. *Chem. Mater.* **2001**, *13*, 2979.
19. Fornes, T. D.; Yoon, P. J.; Paul, D. R. *Polymer* **2003**, *44*, 7545.
20. Cui, L.; Khramov, D. M.; Bielawski, C. W.; Hunter, D. L.; Yoon, P. J.; Paul, D. R. *Polymer* **2008**, *9*, 3751.
21. Gilman, J. W.; Awad, W. H.; Davis, R. D.; Shields, J.; Harris, R. H., Jr.; Davis, C.; Morgan, A. B.; Sutto, T. E.; Callahan, J.; Trulove, P. C.; DeLong, H. C. *Chem. Mater.* **2002**, *14*, 3776.
22. Costache, M.; Heidecker, M.; Manias, E.; Gupta, R.; Wilkie, C. *Polym. Degrad. Stab.* **2007**, *92*, 1753.
23. Byrne, C.; McNally, T. *Macromol. Rapid Commun.* **2007**, *28*, 780.
24. Livi, S.; Duchet-Rumeau, J.; Pham, T.; Gerard, J. F. *J. Colloid. Interface Sci.* **2010**, *349*, 424.
25. Pucci, A.; Liuzzo, V.; Melai, B.; Pomelli, C. S.; Chiappe, C. *Polym. Int.* **2012**, *61*, 426.
26. Singla, P.; Mehta, R.; Upadhyay, S. N. *Green Sustain. Chem.* **2012**, *2*, 21.
27. Gilman, J. W. *Appl. Clay Sci.* **1999**, *15*, 31.
28. Kashiwagi, T.; Harris, R. H.; Zhang, X., Jr.; Briber, R. M.; Cipriano, B. H.; Raghavan, S. R.; Awad, W. H.; Shields, J. R. *Polymer* **2004**, *45*, 881.
29. Qin, H.; Su, Q.; Zhang, S.; Zhao, B.; Yang, M. *Polymer* **2003**, *44*, 7533.
30. Gilman, J. W.; Jackson, C. L.; Morgan, A. B., Jr.; Harris, R. H. *Chem. Mater.* **2000**, *12*, 1866.
31. Hu, Y.; Wang, S. F.; Ling, Z. H.; Zhuang, Y. L.; Chen, Z. Y.; Fan, W. C. *Mater. Eng.* **2003**, *288*, 272.
32. Dasari, A.; Yu, Z. Z.; Mai, Y. W.; Liu, S. L. *Nanotechnology* **2007**, *18*, 445602.
33. Zhang, J.; Lewin, M.; Pearce, E.; Zammarano, M.; Gilman, J. W. *Polym. Adv. Technol.* **2008**, *19*, 928.
34. Sheng, F.; Tang, X. Z.; Zhang, S.; Ding, X.; Yu, Z. Z.; Qiu, Z. *Polym. Adv. Technol.* **2012**, *23*, 137.
35. Kwon, Y. J.; Kim, D. K.; Kim, W. N.; Cho, B. G.; Hong, S. M.; Koo, C. M. *J. Appl. Polym. Sci.* **2012**, *124*, 2814.
36. Crosthwaite, J. M.; Muldoon, M. J.; Dixon, J. K.; Anderson, J. L.; Brennecke, J. F. *J. Chem. Thermodyn.* **2005**, *37*, 559.
37. Song, L.; Hu, Y.; Yong, Y.; Zhang, R.; Chen, Z.; Fan, W. *Polym. Degrad. Stabil.* **2005**, *87*, 111.
38. Kiliaris, P.; Papaspyrides, C. D. *Prog. Polym. Sci.* **2010**, *35*, 902.
39. Braun, U.; Schartel, B.; Fichera, M. A.; Jäger, C. *Polym. Degrad. Stabil.* **2007**, *92*, 1528.